Solid-state kinetics from time-resolved *in situ* XAFS investigations: reduction and oxidation of molybdenum oxides

T. Ressler*, R.E. Jentoft, J. Wienold, O. Timpe

Fritz-Haber-Institut der Max-Planck-Gesellschaft,
Department of Inorganic Chemistry
Faradayweg 4-6, D-14195 Berlin, Germany
E-mail: Ressler@fhi-berlin.mpg.de

The reduction of MoO_3 with hydrogen was studied by in situ X-ray absorption spectroscopy. The experiments performed focused on elucidating phase composition and evolution with time under isothermal reduction conditions. From temperature programmed experiments short-range structural details about the early stage of the reduction were obtained.

Keywords: molybdenum oxide, time-resolved XAFS, solid state kinetic, reduction, bronze

1. Introduction

The reducibility of MoO_3 or molybdenum mixed oxides has been subject to numerous studies in the past (Arnoldy *et al.* 1985, Ressler *et al.* 2000 and references therein). For the reduction of MoO_3 and formation of MoO_2, Arnoldy et al. postulated a one-step mechanism ($MoO_3 \rightarrow MoO_2$). However, until recently (Ressler *et al.* 2000) the existence of intermediates in the reduction of MoO_3 to MoO_2 was subject to debate. The early stage of the reduction of MoO_3 prior to the formation of MoO_2 was investigated by Thöni and Hirsch (1976) and Gai (1981). The authors proposed that oxygen vacancies originating in the course of reduction resulted in the formation of shear-planes in molybdenum trioxide. In order to further elucidate the mechanism of MoO_3 reduction in particular structural changes during the early stage of reduction, we have performed in situ time-resolved XAFS studies on the reducibility of MoO_3 under different H_2 partial pressures and under isothermal as well as temperature programmed reaction conditions.

2. Experimental

2.1 MoO_3 preparation and characterization

Molybdenum trioxide (MoO_3) was prepared by thermal decomposition of ammonium heptamolybdate (AHM), $(NH_4)_6Mo_7O_{24}\cdot 4H_2O$ (*Aldrich Co.*), in He (RT – 773 K, 2 K/min) followed by oxidation in flowing synthetic air at 773 K for 2 h.

2.2 In situ X-ray Absorption Spectroscopy

For in situ XAFS experiments molybdenum oxide was mixed with boron nitride (ratio 1:3) and 30 mg of the mixture was pressed with a force of 1 ton into a 5 mm diameter self-supporting pellet. The absorption jump, $\Delta\mu x$, at the Mo K edge was ~ 2. In situ XAS experiments were carried out in transmission in a flow-reactor at atmospheric pressure. Reaction temperature and reactant mass flow were controlled with an *Eurotherm* PID temperature controllers and *Bronkhorst* mass flow controller, respectively. Temperature programmed reduction or reaction experiments were conducted in flowing reactants (20 ml/min) at a constant heating rate of 5 K/min. The product composition at the in situ cell gas outlet was continuously monitored using a mass spectrometer in a multiple ion detection mode (QMS200 from *Pfeiffer*). In situ transmission XAS experiments were carried out at the Mo K edge (19.999 keV) at beamline X1.1 at the *Hamburger Synchrotron Radiation Laboratory*, HASYLAB, utilizing a Si(311) double crystal monochromator in the Quick-EXAFS mode (Frahm, 1988) (measuring time ~ 4 min/scan). Time-resolved in situ XAS experiments were carried out at the Mo K edge utilizing an energy-dispersive spectrometer (*European Synchrotron Radiation Facility*, ESRF, ID24 (Hagelstein *et al.*, 1997)) equipped with a curved Si(111) polychromator in a transmission mode (measuring time ~ 3 s/scan).

2.3 XAFS Data Analysis

Details on data reduction procedures for energy-dispersive X-ray absorption spectra (i.e. energy calibration, etc.) can be found in references (Ressler *et al.* 1997). X-ray absorption fine structure (XAFS) analysis was carried out using the software package WinXAS v2.0 (Ressler, 1998) following recommended procedures from the literature (Koningsberger und Prins, 1988). Background subtraction and normalization were performed by fitting linear polynomials to the pre-edge and the post-edge region of an absorption spectrum, respectively. The Mo K edge absorption threshold was determined from the first root in the first derivative of the near-edge region (XANES) (in the following edge shifts are reported relative to the first inflection point in the Mo metal K edge XANES at 19999 eV). Principal component analysis (PCA, a.k.a. "factor analysis") of the XANES region was utilized to identify Mo oxide phases present during the reduction and re-oxidation of MoO_3. Given a set of molybdenum reference spectra, PCA can identify those references that constitute probable components in the original set of experimental XANES spectra. Subsequently, after determination of the number and type of phases present, a least-squares fitting procedure can be applied to obtain the fraction of each reference phase under oxidation/reduction conditions. Details on PCA analysis and the numerical procedures employed can be obtained from the literature (Ressler *et al.*, 2000). A smooth atomic background, $\mu_0(k)$, was obtained using cubic splines. The radial distribution function $FT(\chi(k))$ was obtained by Fourier transforming the k^3-weighted experimental $\chi(k)$ function, multiplied by a Bessel window, into the R space. EXAFS data analysis was carried out using theoretical backscattering phases and amplitudes calculated with the ab-initio multiple-scattering code FEFF7 (Rehr et al., 1994). Details about the fitting procedure employed can be found in (Ressler et al., 1999).

3. Results and Discussion

Figure 1 displays a series of Mo K near-edge spectra measured during reduction and reoxidation of MoO_3 at 823 K with hydrogen and oxygen, respectively. The XANES spectra were measured over a period of 10 min with a time resolution of 2.8 s per spectrum. The noticeable increase or decrease in the first Mo K edge absorption feature corresponds to a reduction or oxidation of molybdenum, respectively. Principal component analysis of XANES spectra measured during reduction of MoO_3 in pure hydrogen at 823 K revealed three primary components to be present in the experimental XANES data. By means of target transformation the three oxides MoO_3, MoO_2, and monoclinic Mo_4O_{11} were found to be suitable references. Figure 2 shows the results of a quantitative phase analysis of Mo K near-edge spectra measured during the reduction of MoO_3 at 823 K. After an "induction period" the formation of Mo_4O_{11} can be seen prior to the formation of MoO_2. A complete conversion of MoO_3 to a mixture of MoO_2 and Mo_4O_{11} can be observed after ~ 5 min and a complete reduction of MoO_3 to MoO_2 after ~ 15 min under the conditions employed. Furthermore, it can be seen that the reoxidation proceeded much more rapidly than the reduction and appears to be only gas transport limited. During the reoxidation of MoO_2 the formation of Mo_4O_{11} can also be observed. From XAFS experiments carried out at temperatures below 773 K (50 vol-% to 100 vol-% hydrogen) it was found that the reduction of MoO_3 did not result in the formation of any detectable well-defined molybdenum suboxide phases. A one-step reduction of MoO_3 to MoO_2 was observed in these cases.

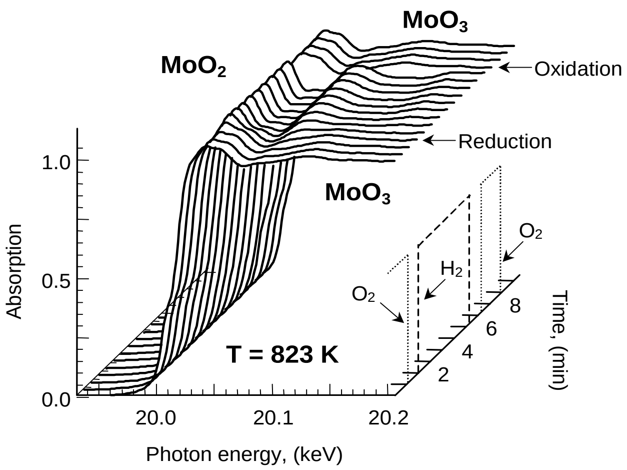

Figure 1
Evolution of Mo K edge XANES spectra during reduction and reoxidation of MoO_3 at 823 K in 100 vol-% H_2 and 100 vol-% O_2, respectively. The normalized mass signals of H_2 and O_2 are schematically depicted. The majority phases MoO_3 and MoO_2 are indicated.

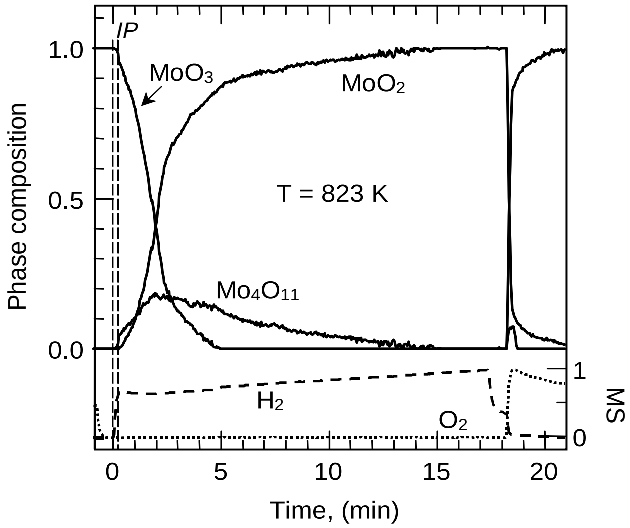

Figure 2
Evolution of phase composition during reduction (100 vol-% H_2) and reoxidation (100 vol-% O_2) of MoO_3 at 823 K. The number and type of phases present (i.e. MoO_3, MoO_2, and Mo_4O_{11}) were determined by PC analysis. The amount of each phase was obtained from a least-squares fit of reference spectra to the corresponding experimental XANES spectra. Hydrogen (*dashed*) and oxygen (*dotted*) mass signals are shown. A short induction period (IP) can be seen in the reduction of MoO_3.

Taking these results and the corresponding XRD experiments (Ressler *et al.*, 2000) into account, it seems that the formation of the well-defined suboxide Mo_4O_{11} in the course of the reduction of MoO_3 with hydrogen is not due to a two step reduction mechanism but rather due to a parallel reaction of the product MoO_2 with unreacted MoO_3. Apparently, a competition between the reduction of MoO_3 and the formation of Mo_4O_{11} can be assumed. At low hydrogen concentration (< 10 vol-%) and temperatures above 698 K the relatively slow rate of reduction permits the formation of well-ordered crystalline Mo_4O_{11}; at increased hydrogen concentrations, though, the rapidly proceeding MoO_3 reduction to MoO_2 or Mo metal prevents the formation of crystalline Mo_4O_{11}. Also, the formation of Mo_4O_{11} during reoxidation is in agreement with its formation during reduction, namely that it is formed in a parallel reaction from MoO_3 and MoO_2.

Least-squares refinements of the Avrami-Erofeev equation (Ressler *et al.*, 2000) to the sigmoidal evolution of the MoO_3 phase measured in isothermal reduction experiments were employed to determined MoO_3 reduction rate constants k_{MoO3}. For the reduction of MoO_3 in 40 % hydrogen without parallel formation of Mo_4O_{11} an apparent activation energy of E_A = 34 kJ/mol is obtained, whereas for the reduction of MoO_3 in 5 vol-% hydrogen, an apparent activation energy of E_A = 133 kJ/mol is obtained. Evidently, the apparent activation energy of the reduction of MoO_3 in hydrogen is dependent on the H_2 partial pressure.

In situ XAFS measurements were performed during temperature-programmed reduction (TPR) of MoO_3 in 50 % H_2 (4 min/scan, heating rate of 5 K/min) to elucidate bulk structural changes in MoO_3 during the early stage of the reduction with hydrogen. The corresponding radial distribution functions, FT(χ(k)), are displayed in Figure 3.

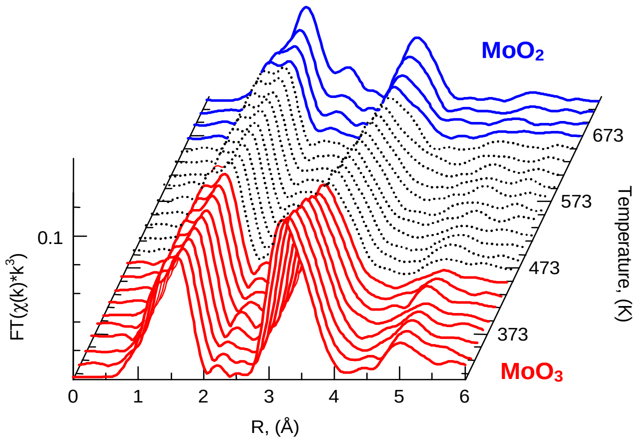

Figure 3
Evolution of Fourier transformed χ(k) of the Mo K edge during temperature-programmed reduction of MoO_3 with 50 % hydrogen. Prior to the formation of MoO_2 at ~ 673 K (473 K - 673 K) a continuous change in the first Mo-O shells can be seen.

In the temperature range from 473 K to 673 K a change in the first Mo - O shells is visible, which can not be attributed to the increasing temperature. At 673 K the onset of the formation of MoO_2 can be seen. Figure 4 shows the evolution of the phase composition (MoO_3 and MoO_2) together with the relative Mo K edge-shift obtained from a XANES analysis of the corresponding spectra in Figure 3. Prior to the formation of MoO_2 (473 K - 673 K) a slight shift of the Mo K-edge towards lower photon energies can be seen, indicating an ongoing reduction of MoO_3 in this temperature range without the formation of a distinct and ordered new phase. A refinement of theoretical EXAFS χ(k) of orthorhombic MoO_3 to the experimental spectra in Figure 3 afforded the evolution of Mo - O distances within the first coordination sphere around the Mo absorber during TPR of MoO_3 (Figure 5). In comparison to the anisotropic expansion of the first Mo - O shells obtained for the treatment of MoO_3 in helium (Figure 5) a considerable deviation from the regular thermal expansion can be seen at 473 K.

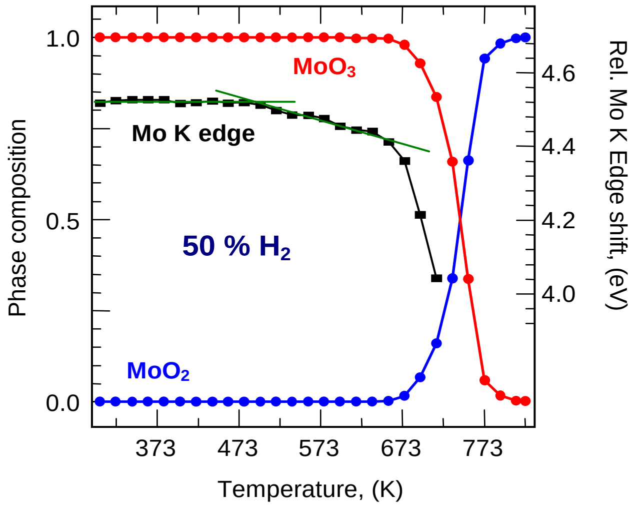

Figure 4
Evolution of phase composition (MoO_3 and MoO_2) and relative Mo K edge shift during temperature programmed reduction of MoO_3. Prior to the formation of MoO_2 at 673 K an edge-shift towards lower photon energies can be seen.

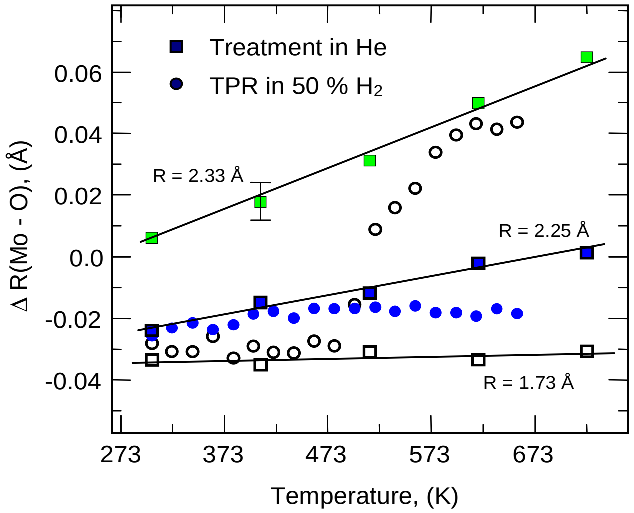

Figure 5
Evolution of selected Mo - O distances (relative to the crystallographic data of orthorhombic MoO_3) in the first coordination sphere (distorted MoO_6 octahedron) around the Mo absorber during temperature programmed reduction of MoO_3 with 50 % H_2 (circles) and temperature treatment of MoO_3 in helium (squares). The anisotropic expansion of MoO_3 (c-direction, perpendicular to MoO_3 layers) is in excellent agreement with in situ XRD experiments.

In total, these results indicate that in the early stage of the reduction of MoO_3 and prior to the formation of MoO_2, hydrogen is incorporated into the lattice. This results in a slight reduction of molybdenum (Mo K edge shift) and a distortion of the first coordination sphere around the Mo absorber. However, the basic layer structure of orthorhombic MoO_3 is preserved and no crystallographically well-defined molybdenum bronzes are being formed during this process. The incorporation of hydrogen into the MoO_3 lattice on the other hand can explain the H_2 concentration-dependent apparent activation energy observed for the reduction of MoO_3.

4. Conclusion

Phase composition and evolution with time during isothermal reduction of MoO_3 with hydrogen was studied by in situ X-ray absorption spectroscopy. A one step reduction process ($MoO_3 \rightarrow MoO_2$) was established. Formation of the molybdenum suboxide Mo_4O_{11} from a parallel reaction of MoO_3 and MoO_2 at temperatures above 700 K was found. During temperature programmed reduction of MoO_3 the formation of a molybdenum bronze (H_xMoO_3) was observed prior to the detection of MoO_2.
The results presented demonstrate the potentials of time-resolved in situ XAFS. From XAFS spectra measured with a time-resolution of several seconds to several minutes both the XANES and the EXAFS region can be used to reveal phase composition, kinetics, and short-range structural information of solid state reactions.

5. Acknowledgement

We acknowledge the *Hamburger Synchrotron Radiation Laboratory* (L. Tröger), HASYLAB, and the *European Synchrotron Radiation Facility* (T. Neisius), ESRF, for providing beamtime for this work. TR thanks the *Deutsche Forschungsgemeinschaft*, DFG, for financial support (Habilitationsstipendium). The authors are very grateful to Prof. Dr. R. Schlögl for fruitful discussions and support.

References:

Arnoldy, P.; de Jonge, J.C.M.; Moulijn, J.A. (1985) *J. Phys. Chem.* 89, 4517.
Frahm, R., (1988) *Nucl. Instrum. Meth.* A270, 578.
Hagelstein, M.; San Miguel, A.; Fontaine, A.; Goulon, J. (1997) *J. de Physique IV* 7, C2-303.
Gai, P.L. (1981) *Philos. Mag.* 43, 841.
Koningsberger, D. C.; Prins (1988) R. *X-ray Absorption Spectroscopy, Chemical Analysis, 92,* Wiley, New York.
Rehr, J. J.; Booth, C. H.; Bridges, F.; Zabinsky, S. I. (1994) *Phys. Rev. B* 49, 12347.
Ressler, T.; Jentoft, R.E.; Wienold, J.; Günter, M.M.; Timpe, O. (2000) *J. Phys. Chem. B* 104, 6360-6370.
Ressler, T.; Hagelstein, M.; Hatje, U.; Metz, W. (1997) *J. Phys. Chem. B* 101, 6680.
Ressler, T. (1998) *J. Synch. Rad.* 5, 118-122.
Ressler, T.; Wong, J.; Roos J.; Smith, I.L. (2000) *Environ. Science & Techn.*, 34, 950-958.
Ressler, T.; Brock, S.L.; Wong, J.; Suib, S.L. (1999) *J. Phys. Chem. B*, 103, 6407-6420.
Thöni, W.; Hirsch, P.B. (1976) *Philos. Mag.* 33, 639.

Received 31 July 2000 • Accepted 30 October 2000